Available online at www.sciencedirect.com
SCIENCE DIRECT®
European Polymer Journal 40 (2004) 1001–1011
EUROPEAN POLYMER JOURNAL
www.elsevier.com/locate/europolj

Probing polymers with single fluorescent molecules

Nikodem Tomczak [a,b], Renaud A.L. Vallée [a,b,1], Erik M.H.P. van Dijk [b], Maria García-Parajó [b], Laurens Kuipers [b], Niek F. van Hulst [b,*], G. Julius Vancso [a,*]

[a] *Department of Materials Science and Technology of Polymers, Faculty of Science and Technology, University of Twente, MESA+ Institute for Nanotechnology, P.O. Box 217, 7500 AE Enschede, The Netherlands*
[b] *Applied Optics Group, Faculty of Science and Technology, University of Twente, MESA+ Institute for Nanotechnology, P.O. Box 217, 7500 AE Enschede, The Netherlands*

Received 2 December 2003; received in revised form 16 January 2004; accepted 20 January 2004

Abstract

The use of single molecules to study local, nanoscale polymer dynamics is presented. Fluorescence lifetime fluctuations were used to extract the number of polymer segments (N_s) taking part in the rearranging volume around the probe molecule below the glass transition temperature. N_s was dependent on the temperature and it decreased with increasing temperature. Above the glass transition, rotational motion of single molecules was followed in time and typical time-scales of the rotational diffusion were extracted. These two approaches allowed us to obtain non-averaged information about the heterogeneous dynamics present in polymer systems, on the nanoscale, above and below glass transition temperatures.

Keywords: Single molecules; Fluorescence lifetime; Rotational diffusion; Heterogeneous dynamics

1. Introduction

Photophysics and photochemistry in polymer science has been one of central areas of interest for a long time [1]. *Single molecule* fluorescence detection (SMD) is a newly developed optical technique with its major strength laying in the intrinsic ability to avoid ensemble averaging [2–7]. By looking at one particular chromophore within a population it is possible to directly determine how the particular chromophore participates in the ensemble averaged behavior. Related experiments allow one to tackle phenomena which otherwise would be hidden, or would be difficult to access [8]. The typical nanometer scale dimensions of the chromophoric probes and the well-developed instrumentation [9,10] make SMD an indisputably valuable tool in biology [11–16], chemistry [17–19] and physics [20,21], which allows one to look at microscopic processes, which take place on the nanometer scale.

Much attention has been paid to studies of dynamics of polymers in the glassy and viscoelastic states due to their relevance in microelectronics [22], lithography [23] or nanocomposites [24,25]. The glass transition phenomenon, although known for a long time, is still not fully understood [26–28]. Single molecule methods are promising candidates to resolve the controversies present in this field e.g. the length scales and time scales involved in the spatially heterogeneous dynamics [29] or the effects of confinement on the dynamics of macromolecules [30,31]. One spectacular example of using the

* Corresponding authors. Tel.: +31-53-489-3172; fax: +31-53-489-3511 (N.F. van Hulst), tel.: +31-53-489-2967; fax: +31-53-489-3823 (G. Julius Vancso).
E-mail addresses: n.f.vanhulst@tnw.utwente.nl (N.F. van Hulst), g.j.vancso@utwente.nl (G. Julius Vancso).
[1] Present address: Department of Chemistry, Catholic University of Leuven, Celestijnenlaan 200 F, B-3001 Leuven, Belgium.

0014-3057/$ - see front matter © 2004 Elsevier Ltd. All rights reserved.
doi:10.1016/j.eurpolymj.2004.01.045

single-molecule method is the confirmation of the reptation model for polymer diffusion by direct observation of a single diffusing macromolecule labeled with fluorescent dyes [32,33]. This constitutes a result, which could have never been achieved using bulk, ensemble averaged methods. Single-molecule fluorescence approaches were also employed to probe crystals of organic molecules [34] and glassy materials [35] and related results have significantly contributed to the understanding of structure and dynamics of soft condensed matter. Lattice dynamics at low temperatures was investigated by following single molecule spectral diffusion or linewidth distributions and different explanations based on a two-level-system concept [36,37] were developed to account for the observed behavior [38–41].

Although experiments at cryogenic conditions give a vast amount of information about the host, most of the common use materials have working temperatures close to room temperature. In such conditions thermal fluctuations are large and, therefore, most of the phenomena that were observed at low temperature cannot be resolved. At room temperature, using near-field optical microscopy, lateral diffusion and dynamic reorientation of single rhodamine dyes embedded in poly(vinylbutyral) was monitored. Non-random diffusion was revealed in these studies on the microscopic scale while time-averaged macroscopic diffusion was shown to display random-walk behavior [42,43]. Using confocal fluorescence microscopy, heterogeneous dynamics in polymer films was examined by monitoring the rotational motion of single molecules in the melt few degrees above the glass transition [44–46]. Inhomogeneity of the host matrix was found by observing a bimodal distribution of fluorescence lifetimes for a flexible triphenylmethane dye derivative in poly(methyl methacrylate) (PMMA) [47,48]. Results were explained by changes of the non-radiative component of the fluorescent decays due to the interaction of the dyes with different sites in the polymer matrix. Similar "bimodal" distributions were found for the radiative component of the fluorescence lifetime of single perylene dye in PMMA [49] and were explained by assuming switching of the dye between two different conformations with rate controlled by the interactions of the probe with the surroundings. Chemical heterogeneity of a silica sol–gel was also probed by looking at the mobility and photostability of single carbocyanine molecules [50]. Another approach to look at the dynamics of the host consisted of attaching the chromophores to the polymeric chain at different locations. This allowed to probe directly the dynamics of single polymer chains in a host matrix of different (or of the same) material [51]. In many of the aforementioned studies spatial and temporal heterogeneities were observed and their role in the overall physicochemical behavior was deciphered for materials and systems, which appeared homogeneous on the ensemble detection level.

In this contribution we describe two different single molecule fluorescence methods, which are used to investigate polymer dynamics in the glassy and viscoelastic states. The first method [52] is based on *fluorescence lifetime fluctuations* of a dicarbocyanine dye. This powerful technique makes possible the observation of density fluctuations in the polymer matrix on the nanometer scale far *below* the glass transition temperature of the polymer. The second method relies on the monitoring of single molecule *reorientational diffusion* of a rhodamine dye in a polymer *above* its glass transition temperature. Broad range of time-scales for diffusion is observed and different mechanisms of reorientation of the probe are witnessed. Heterogeneous dynamics is shown to be present close to the glass transition and persists far below T_g.

2. Experimental section

Materials and sample preparation. The probes used in this study were DiD (1,1′-dioctadecyl-3,3,3′,3′-tetramethylindodicarbocyanine perchlorate, Molecular Probes D-307) and 5-TRITC (tetramethylrhodamine-5-isothiocyanate, G isomer, Molecular Probes T-1480). As host matrices we chose polystyrene (PS, $M_n = 89{,}300$ g/mol, $M_w/M_n = 1.06$, Polymer Standard Service, $T_g = 100$ °C), poly(isobutyl methacrylate) (PIBMA, $M_n = 67{,}200$ g/mol, $M_w/M_n = 2.8$, prepared in our laboratories by custom-free radical polymerization, $T_g = 56$ °C) and poly(methyl acrylate) (PMA, $M_n = 120{,}000$ g/mol, Aldrich, $T_g = 8$ °C). The chemical structures of the chromophores and polymers are presented in Fig. 1. Solutions of the dyes in toluene (for DiD) or in tetrahydrofuran (THF, for 5-TRITC) containing different amounts of polymer were spin-coated at 3000 rpm for 60 s onto a cleaned glass cover slides (with a diameter of 10 or 20 mm, Fisher Scientific) to produce uniform thin

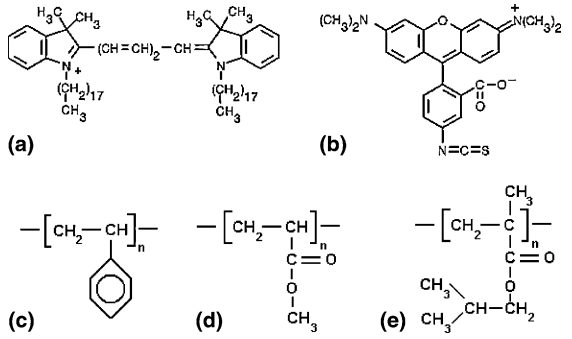

Fig. 1. Chemical structures of probe molecules: DiD (a), 5-TRITC (b), which were embedded in polymer matrices: PS (c), PMA (d) and PIBMA (e).

coatings with thickness values ranging from 10 to 300 nm. Changing the concentration of the polymer in the solution varied the thickness as anticipated [53]. The concentration of the dyes in the resulting films was kept low enough (10^{-9}–10^{-10} M) to ensure adequate spatial separation for optical single molecule observations. The samples were subsequently annealed in vacuum, first 12 h at 60 °C and later 3 h at 105 °C. A DiD/polystyrene sample with a higher concentration of dye (10^{-6} M) was also prepared for calibration purposes. Atomic Force Microscopy (Nanoscope III, Digital Instruments, Santa Barbara) was used to determine the planarity and roughness (<1 nm) of the samples. Film thickness values were determined by a "tip-scratch" [54,55] method. Corresponding thickness values were also determined by ellipsometry for the sake of comparison. The difference between the two methods was found to be less than 3%.

Scanning confocal microscopy (SCM) and time resolved fluorescence. A picosecond-pulsed dye laser (635 nm, PicoQuant, 800-B, 100 mW) with a repetition rate of 80 MHz was used for excitation. The excitation light was made circularly polarized by using a $\lambda/4$ plate and focused onto the sample to a diffraction-limited spot using an air objective (Olympus, NA = 0.75). To separate the fluorescence emission from the excitation, suitable dichroic mirrors, emission and excitation filters, were used. Fluorescence photons were collected by the same objective and subsequently focused and collected by two avalanche photodetectors (APD, SPCM-AQ-14, EG&G Electro Optics) placed after a polarization beam splitter. A custom-built piezo-scan table with an active x–y feedback loop mounted on a commercial optical microscope (Zeiss) was used. The sample was scanned over the focus of the excitation spot, producing a two-dimensional fluorescence intensity image for two independent polarization channels. For time resolved experiments the detected fluorescence signal was fed into a time-correlated single-photon counting card (TCSPC, Becker & Hickl, SPC 500). For each single molecule, intensity and fluorescence lifetime traces were collected with 100 ms integration time, during a 20–60 s total observation time. The accuracy of lifetime determination was on the order of 300 ps. Custom LabView software was used to control the scanning process and data acquisition. For higher temperature measurements a home-built heating-stage was placed below the sample and the temperature was monitored during the experiments with an accuracy of ±2 °C.

Wide field microscopy (WFM). Light from a cw Ar^+–Kr^+ ion laser at wavelengths of 531 and 647 nm was used for excitation. Circularly polarized laser beam passed through a beam expander and was focused onto the back aperture of a high NA objective (Zeiss, NA = 1.4, oil immersion). The fluorescence photons emitted from the illuminated area were collected by the same objective and after passing through emission filters were split into two orthogonal polarization channels using a Wollaston prism (Linos 037808) and subsequently imaged with a 500 mm lens (Linos 063827) onto an intensified charged coupled device (CCD camera, Pentamax GEN IV). The speed of the data acquisition by the camera was set to 100 ms/frame. The images from the camera were processed by custom LabView software. Simultaneous intensity and polarization information from each pixel on the frame were obtained.

3. Results and discussion

Fig. 2a and b show fluorescence intensity images (DiD molecules embedded within a thin PS film) obtained with SCM and WFM, respectively. The fluorescent molecules in the samples are spatially separated and distributed throughout the polymer film as expected from the low dye concentration used to spin the polymer solutions. Separation of the dyes over large distances (hundreds of nanometers) also avoids any interaction between them. The color scale on both

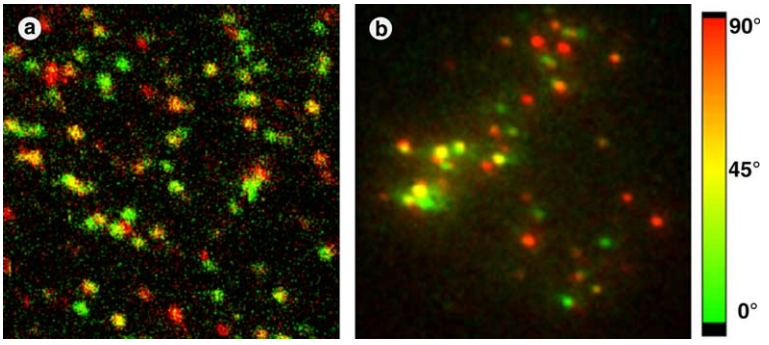

Fig. 2. (a) 10×10 μm^2 fluorescence intensity scan of DiD molecules in PS obtained by SCM, (b) 10×10 μm^2, 100 ms integration time, fluorescence intensity "frame" of DiD molecules in PS obtained by WFM. The visible spots correspond to the fluorescence emitted by single molecules. The color scale is related to the polarization of the collected fluorescence.

pictures is related to the polarization of the detected fluorescence. The constant value of this parameter within the spots indicates that the fluorescence spots are indeed single immobilized molecules. Random distribution of orientations of the dyes in the samples ensures that no specific structure of the films was induced using the preparation procedure (spin-coating). The variation in the intensities between different molecules is mainly related to their degree of out-of-plane orientation, and therefore to excitation and photon collection efficiencies. Intensity variations are also related to different characteristic "nanoenvironments" of the probes, which influence their fluorescence lifetime [56], triplet excursions [57,58] long dark state statistics [59] or absorption and emission spectra [3].

In scanning confocal microscopy the excitation light is focused to a diffraction limited spot. Its size depends on the excitation wavelength and the numerical aperture (NA) of the objective used. The radius of the spot is approximately equal to $\sim\lambda_{ex}/4$ and this determines the spot size on the image in Fig. 2a. Therefore, to obtain a two-dimensional fluorescence image, one must use a scanning stage and move the focused excitation light across the sample in a pixel-by-pixel fashion. Therefore, methods based on scanning lack the ability to observe fast molecular motions on a macroscopic scale, or to monitor simultaneously many molecules separated over large distances. However, small excitation volumes in the diffraction-limited spot improve considerably the signal-to-noise ratio (S/N). In Fig. 2a the S/N for single molecules is equal to $\approx$20. In combination with fast photon detectors, like APDs, scanning confocal microscopy is the technique, which is suitable to monitor processes that require a combination of high spatial and temporal resolution. Fluorescence lifetime determination (in the nanosecond scale) for single molecules falls within these considerations where the time resolution in the order of few hundreds of picoseconds can be obtained. In contrast to SCM, in wide-field microscopy a large area of many microns in diameter is illuminated. However, the resolution is still diffraction limited and its value depends on the quality of the optics used in the experimental setup. The use of fast acquisition devices (like CCD cameras) allows one to perform real-time observations of translational or rotational diffusion of many individual molecules simultaneously. Such studies, where direct determination of the spatial distribution of molecular behavior is possible, are perfectly suited to investigate systems, where spatial heterogeneities (both static and dynamic) are present. The drawback of this method is related to the rather limited time resolution of CCD cameras (down to few milliseconds depending on the size of the pixel array being read out) and to the poorer signal to noise ratios that can be obtained (S/N $\approx$ 8 in the case of Fig. 2b).

3.1. Confocal microscopy and single molecule fluorescence lifetime fluctuations

Following localization of the fluorescence spots in the sample, the excitation focus is shifted to a molecule one wishes to investigate. Once the molecule is in the focus, fluorescence emission can be followed in time and photon time-traces can be registered until photodegradation. In single molecule studies the fluorescence lifetime is often determined using Time-Correlated Single Photon Counting [60] by plotting a histogram of time lags between the excitation pulses and the detected fluorescence photons. The exponential fit to the observed decay profile gives the fluorescence lifetime (τ_f). Binning all of the arrived photons within a defined time-interval produces fluorescence lifetime time-traces. An example for such a time-trace for a single DiD molecule embedded within a 70 nm PS thin film is shown in Fig. 3. While the total fluorescence intensity remains essentially constant for the whole time-trace, the fluorescence lifetime exhibits frequent excursions towards longer values. The τ_f distribution in this case has a clearly visible asymmetric shape (Fig. 3c). The absence of correlation between the intensity and fluorescence (Fig. 3b) rules out the possibility that the observed lifetime fluctuations are due to the opening of new non-radiative channels for the molecule to decay from the singlet excited state to the ground state. Macklin et al. [60], Vallée et al. [61] and Kreiter et al. [62] have shown that the orientation of the transition dipole moment of single molecules with respect to the optical interfaces influences the value of the fluorescence lifetime. However, by monitoring the location of each molecule and the orientation of the transition dipole moment, we found no evidence for orientational or translational motion under the experimental conditions used (far below T_g). Modification of the transition frequency, or the transition dipole moment, can also result in fluorescence lifetime fluctuations. However, it was previously found that the molecular conformations of DiD is similar in the ground and the excited states and that it does not contribute significantly to the observed large fluctuations in τ_f [63]. Therefore, the observed behavior is attributed to the fluctuations present in the local nanoenvironment of the probe. To shed further light on this statement, we start with the expression for the radiative decay rate (inverse of the lifetime) of an excited molecule, in a homogeneous dielectric, in the following form [64]:

$$\Gamma = \frac{4f^2 n}{3\hbar c^3} |\vec{\mu}_{10}|^2 \langle \omega^3 \rangle_{fcf}, \tag{1}$$

where n is the refractive index of the medium, $\hbar$ is the Planck constant divided by 2π, c is the speed of light, f is a factor which relates the macroscopic and local electric fields, $\langle \omega^3 \rangle_{fcf}$ is the Franck-Condon-weighted average of

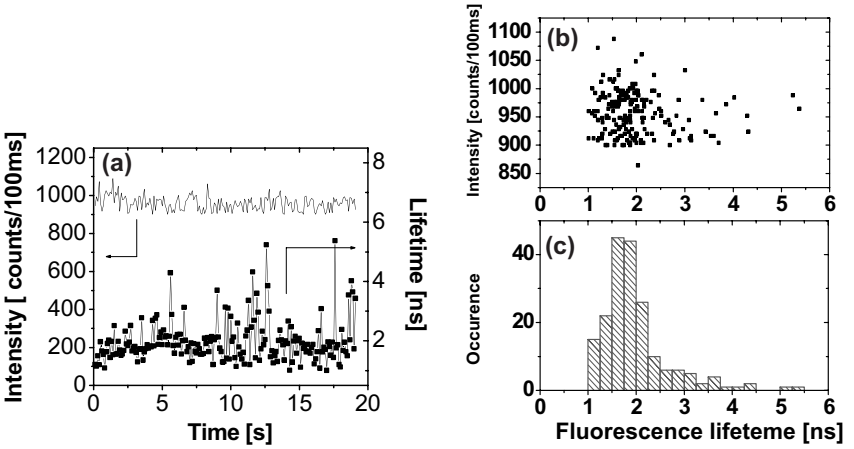

Fig. 3. (a) Fluorescence intensity and lifetime time-traces for a single DiD molecule in PS. Binning time is 100 ms. (b) Correlation between intensity and lifetime. (c) Histogram of lifetimes presented in (a).

the electronic transition frequency and $\vec{\mu}_{10}$ is the transition dipole moment. Although it is usually assumed that the decay rate of a molecule from its excited state is an intrinsic property of the molecule, Eq. (1) explicitly shows that it also depends on the dielectric properties of the surroundings [65] directly through n and indirectly through f [66]. The detailed explanation of the physical meaning of f is outside of the scope of this publication, however it suffices to mention that f relates the macroscopic and microscopic (local) electric fields, which act on the probe and is itself a function of n [67–70]. At the microscopic level, the dielectric host cannot be treated as a continuum and macroscopic concepts like the refractive index are no longer applicable in their common forms. We introduce the effective dielectric constant (ε_{eff}), which depends on the relative fraction of empty space (h) in a polymer lattice model competing with polymer segments $(1-h)$ corresponding to occupied space:

$$\varepsilon_{\text{eff}}(h) = h \cdot \varepsilon_{\text{vac}} + (1-h) \cdot \varepsilon_{\text{pol}}, \tag{2}$$

where ε_{vac} and ε_{pol} is the vacuum and polymer dielectric constants, respectively. In a fluctuating environment the fluorescence lifetime will develop a specific distribution depending on the degree of mobility in the surroundings. Recently, we presented a method [52] to obtain from the lifetime distributions of each molecule the number of polymer segments (N_s), which take part in the cooperatively rearranging volume around the probe by using the Simha–Somcynsky equation of state [71]. Fig. 4 shows a distribution of N_s for many different molecules embedded within the same 70 nm thick PS sample. The broad distribution of N_s indicates that large heterogeneous dynamics of the polymeric matrix is present on the nanoscale level well below the glass transition temperature. Such detailed information related to the microscopic distribution of relaxation rates is otherwise hard or impossible to obtain since only a unique combination of small probed volume and the possibility to obtain non-averaged information can lead to the result presented in Fig. 4. It is interesting to note that N_s is a function of the temperature (Fig. 5). The N_s behavior as a function of temperature is strikingly similar for two different polymers when plotted against the temperature reduced with respect to the glass transition temperature of the polymer used. Such an observation is in agreement with the configurational entropy model of Adam and Gibbs [72] where the size of the cooperatively rearranging regions is predicted to decrease when approaching the glass transition from below.

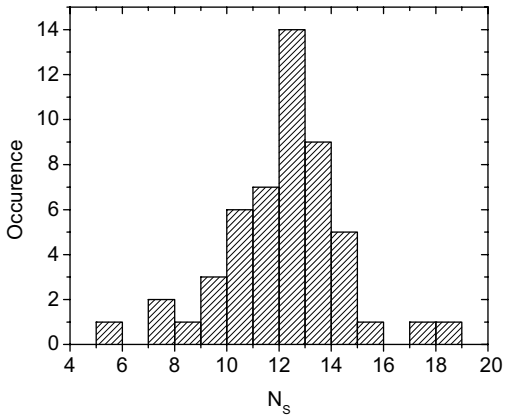

Fig. 4. Distribution of N_s values for 53 DiD molecules embedded in a 70 nm thick PS film at room temperature (80° below T_g).

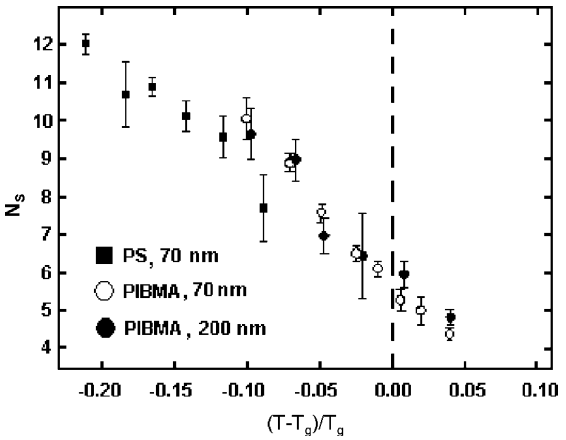

Fig. 5. N_s as a function of reduced temperature. T_g of 56 °C for PIBMA and 100 °C for PS was taken for calculations. A common number of six segments can be found at the glass transition. Reprinted with permission from Vallée RAL, Tomczak N, Kuipers L, Vancso GJ, van Hulst NF. Phys Rev Lett 2003;91(3):038301. © 2003 American Physical Society [52].

3.2. Wide-field microscopy and rotational dynamics

As it was already mentioned, WFM allows one to obtain 2-D fluorescence images (“frames”) of many single molecules simultaneously (Fig. 2b). Time-dependent information is extracted by following the intensity of each individual molecules “frame” after “frame”. This allows one to construct fluorescence intensity traces for two independent polarization directions for each pixel, or group of pixels. From these time-traces we then obtain information about the orientational behavior of single molecules. Fig. 6a shows a time-trace for a single 5-TRITC molecule embedded in a thin (~100 nm) PMA film at room temperature. The total fluorescence intensity fluctuates in time reflecting the changes in the time-dependent emission properties of the molecule and possible out-of-plane rotational motion of the molecule. Correlated signal in the two polarization channels is then visible. Nevertheless, in some parts of the trace (one of them indicated by the arrows) anticorrelated intensity

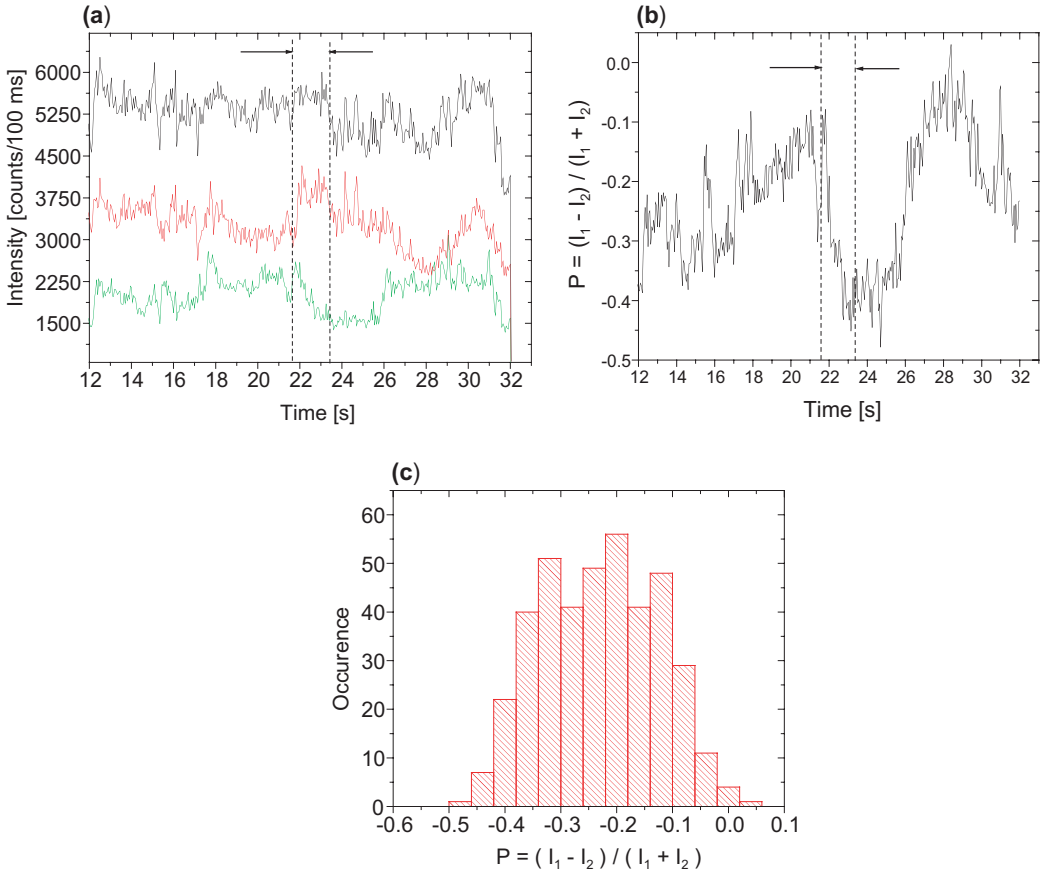

Fig. 6. (a) Total fluorescence intensity (black) and the intensities in the two orthogonal polarization directions (green and red) for a single 5-TRITC molecule in PMA. (b) Degree of polarization (P) calculated using Eq. (3). The arrows in Fig. 6(a) and (b) indicate where rotational motion occurred for this molecule. (c) Static distribution of P values shown in (b).

in the two polarization channels is also observed. Since the total intensity level for that part remains constant, the molecule undergoes in-plane rotational motion.

To estimate the orientation and orientational motion of the probes from single molecule fluorescence intensity time-traces, values of the degree of polarization (P) are calculated (Fig. 6b):

$$P(t) = \frac{I_1(t) - I_2(t)}{I_1(t) + I_2(t)}, \tag{3}$$

where I_1 and I_2 are the intensities in the two orthogonal polarization channels, and t is time. Such a treatment of data ensures that the orientational diffusion probed is not affected by laser intensity fluctuations, or triplet excursions. The values of P can range form -1 to $+1$ with extreme values attainable through a rotation of 90°. Time-trace of P presented in Fig. 6b shows directly that the probe reorients in different directions while being embedded within the polymer matrix. However, not all investigated probes showed clear molecular reorientations. To quantify the extent of molecular mobility of the probes first we classified the molecules as "fixed" or "rotating", during the collection time, by looking at the widths of their static distributions of P (Fig. 6c) [50]. As reference for the "fixed" species we chose the width of the distribution found for DiD molecules in a PS matrix at room temperature (80° below the T_g of PS in the bulk) (not shown here). In such conditions the molecules are (not surprisingly) frozen in the polymer matrix on the timescale of our measurements (minutes). The rotational behavior varied greatly from molecule to molecule within the same sample and even between molecules, which were collected simultaneously on the same frame. Therefore wide-field experiments are spatially mapping the heterogeneous molecular dynamics of the probes inside the polymer above and near to the glass transition. However, due to the far-field characteristic of the detection method, such experiments do not allow to determine accurately the size of the "domains" [29] in which the probe has a particular orientational behavior. We found that 31% of the investigated molecules could be termed as "fixed" and 50% of molecules were termed as "rotating". For the remaining 19% of the molecules extensive hopping behavior was observed and the corresponding time traces exhibited a more complex behavior. An example of a P time-trace of one such molecule is presented in Fig. 7. Regions of slow and fast rotational motions can be distinguished and a significant frequency of orientational jumps is observed. The static distribution of P (Fig. 8) is also broad in this case meaning that the molecule probe many different orientations during the investigation time. However, it does not show one broad peak but rather can be described as a multi-nodal distribution. The red lines in Fig. 7 indicate the values, which correspond to the peak positions

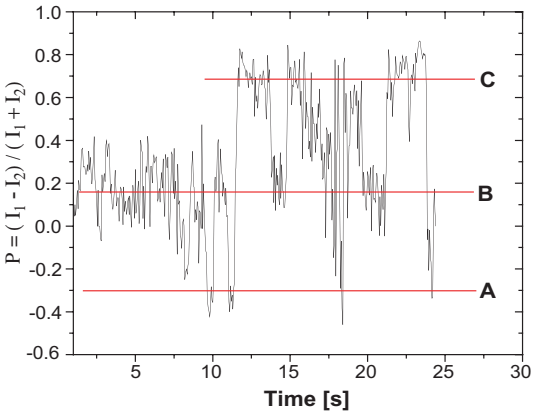

Fig. 7. Time-trace of P for a single 5-TRITC molecule in PMA exhibiting a complex rotational behavior. The red lines are guides to the eyes.

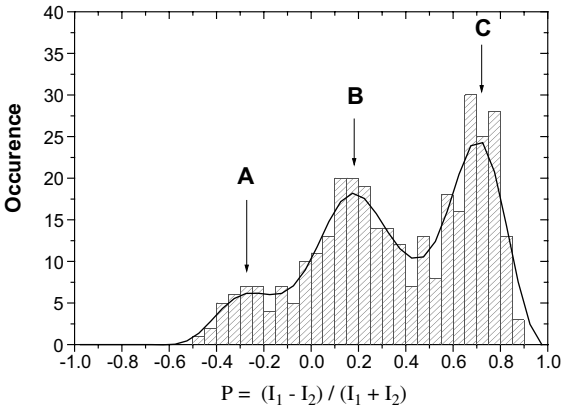

Fig. 8. Static distribution of P presented in Fig. 7. The peak values of P at positions A, B and C are the same as indicated in Fig. 7. The black line is obtained after FFT smoothing of the data.

in the histogram (Fig. 8). A time-trace of P presented in Fig. 7 might suggest that not only the rotational diffusion is mediated by consecutive hopping from one spatial position to another but that it is also the result of hopping between few different orientations (or "sites") within the polymer matrix in which the probe can reside for different amounts of time before switching to another "site" or to start to rotate with different rates. As suggested by Bartko et al. [73] observations of such jumps at the single molecule level can contribute significantly to the understanding of the bulk observations of the translational–rotational paradox near T_g [74]. Such "tumbling" molecules make the extraction of the characteristic timescale of the process to become rather complicated and therefore the molecules exhibiting such behavior are omitted from further analysis.

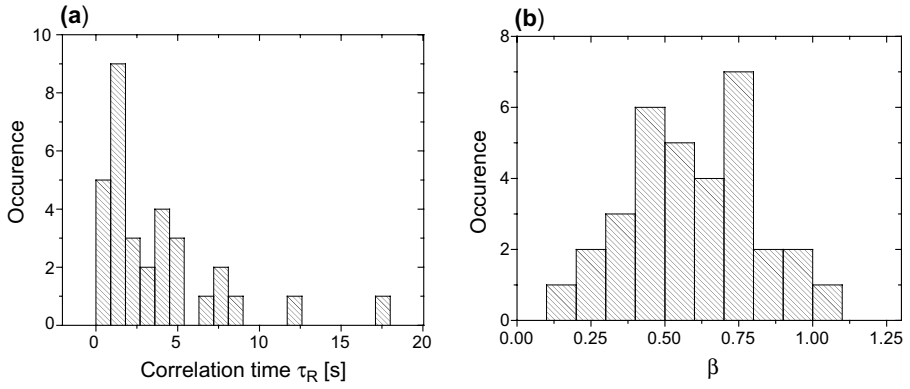

Fig. 9. Histograms of τ_R (a) and β (b) parameters obtained for different single 5-TRITC molecules embedded in the same PMA matrix at room temperature (12° above T_g).

For molecules which do not show extensive hopping, to extract the typical time-scale of the rotational diffusion, the autocorrelation function [$C(t)$] of P was calculated. The shape of $C(t)$ was non-exponential and could be best fitted with the Kohlrausch–Williams–Watt (KWW) equation in the form $C(t) = \exp(-(t/\tau_C)^{\beta})$, where $C(t)$ is the autocorrelation function and τ_C is the characteristic time describing the process. The fitting parameter β determines the shape of the autocorrelation function. This parameter is often called the stretching parameter and its value reflects the breath of the relaxation spectrum ($0 < \beta < 1$; $\beta = 1$ for a single exponential process) [75]. The average rotational correlation time (τ_R) can be directly calculated by integrating $C(t)$ but it can be also obtained by making use of the fitting parameters τ_c and β [75]:

$$\tau_R = \int_0^\infty C(t) = \int_0^\infty \exp\left[-\left(\frac{t}{\tau_C}\right)^{\beta}\right] dt = \frac{\tau_C \Gamma(1/\beta)}{\beta}, \quad (4)$$

where Γ stands for the Gamma function. In Fig. 9a and b we show histograms of τ and β values obtained form many different single molecules. The 5-TRITC molecules, which were called "rotating", exhibit a broad range of rotational time-scales when embedded in the same polymer matrix. In bulk experiments, it was found that the motion of large probes is coupled to the α-relaxation of the polymer chains [76]. For small probes, however, a substantial decoupling from the α-relaxation was found starting at temperatures 30–50° above the glass transition reference [77]. The origins of such a behavior are largely unknown but it has been suggested that smaller probes better couple to the higher order relaxations like the β or γ processes. The relationship between the relaxation times of the probe (τ_R) and the time scale for the relaxation of the polymer chains (τ_{pol}) was described with a relation [78]:

$$\langle \tau_{pol} \rangle = C_i \langle \tau_R \rangle_i^{\xi}, \quad 0 < \xi < 1, \quad (5)$$

where $i = \alpha, \beta, \gamma, \ldots$ and for $\xi = 1$ there is a full coupling to given relaxation process.

Introduction of heterogeneous dynamics found in our single molecule experiments (broad β and τ_R distributions) into Eq. (5) makes the problem more subtle. Describing the system with only an average relaxation time without a proper knowledge of the exact shape of the distribution of the relaxation times might lead to false conclusions. Additional single molecule experiments using probes with different dimensions, chemistry and performed at different temperatures might give the answer for the decoupling mechanism. Such studies are in progress.

4. Conclusions

Single molecule fluorescence methods became powerful tools to probe structure and dynamics of polymers on the nanoscale. Dynamic heterogeneities can be obtained directly by observing distribution of particular properties probed locally by individual probes. Future work will concentrate on the development of microscopic theories of polymer dynamics and its applications to current topics in macromolecular physics like the effect of confinements, structure and dynamics of electronic polymers or protein folding.

Acknowledgements

The authors are grateful to Jeroen Korterik and Frans Segerink for technical support. Hugo van Bergen

is acknowledged for experimental work with WFM. The Council for Chemical Sciences of the Netherlands Organization for Scientific Research (NWO-CW) is acknowledged for financial support of this research. E.v.D. is financed by FOM, Dutch Foundation for Fundamental Research of Matter.

References

[1] Guillet JE. Polymer photophysics and photochemistry: An introduction to the study of photoprocesses in macromolecules. Cambridge: Cambridge University Press; 1985.
[2] Nie SM, Chiu DT, Zare RN. Probing individual molecules with confocal fluorescence microscopy. Science 1994; 266:1018–21.
[3] Xie SX. Single-molecule spectroscopy and dynamics at room temperature. Acc Chem Res 1996;29(12):598–606.
[4] Moerner WE, Orrit M. Illuminating single molecules in condensed matter. Science 1999;283:1670.
[5] Ambrose WP, Goodwin PM, Jett JH, Van Orden A, Werner JH, Keller RA. Single molecule fluorescence spectroscopy at ambient temperatures. Chem Rev 1999; 99(10):2929–56.
[6] García-Parajó M, Veerman JA, Bowhuis R, Vallée RAL, van Hulst NF. Optical probing of single fluorescent molecules and proteins. Chem Phys Chem 2001;2(6):347–60.
[7] Moerner WE. A dozen years of single-molecule spectroscopy in physics, chemistry, and biophysics. J Phys Chem B 2002;106(5):910–27.
[8] Moerner WE. Examining nanoenvironments in solids on the scale of a single, isolated impurity molecule. Science 1994;265:46–53.
[9] Moerner WE. Methods of single-molecule fluorescence spectroscopy and microscopy. Rev Sci Instr 2003;74(8): 3597–619.
[10] Bohmer M, Enderlein J. Fluorescence spectroscopy of single molecules under ambient conditions: methodology and technology. Chem Phys Chem 2003;4(8):793–808.
[11] Tokunaga M, Kitamura K, Saito K, Iwane AH, Yanagida T. Single molecule imaging of fluorophores and enzymatic reactions achieved by objective-type total internal reflection fluorescence microscopy. Biochem Biophys Res Comm 1997;235(1):47–53.
[12] Pierce DW, Hom-Booher N, Vale RD. Imaging individual green fluorescent proteins. Nature 1997;388:338.
[13] Wiess S. Fluorescence spectroscopy of single biomolecules. Science 1999;283:1676–83.
[14] Peterman EJG, Brasselet S, Moerner WE. The fluorescence dynamics of single molecules of green fluorescent proteins. J Phys Chem A 1999;103(49):10553–60.
[15] Byassee TA, Chan WCW, Nie SM. Probing single molecules in single living cells. Anal Chem 2000;72(22):5606–11.
[16] García-Parajó MF, Koopman M, van Dijk EMHP, Subramaniam V, van Hulst NF. The nature of fluorescence emission in the red fluorescent protein DsRed, revealed by single-molecule detection. Proc Nat Acad Sci 2001; 98(25):14392–7.
[17] Trabesinger W, Schutz GJ, Gruber HJ, Schindler H, Schmidt T. Detection of individual oligonucleotide pairing by single-molecule microscopy. Anal Chem 1999;71(1): 279–83.
[18] Zhang P, Tan WH. Direct observation of single-molecule generation at a solid–liquid interface. Chem-Eur J 2000; 6(6):1087–92.
[19] Ha T, Xu J. Photodestruction intermediates probed by an adjacent reporter molecule. Phys Rev Lett 2003;90(22): 223002.
[20] Hettich C, Schmitt C, Zitzmann J, Kuhn S, Gerhardt I, Sandoghdar V. Nanometer resolution and coherent optical dipole coupling of two individual molecules. Science 2002;298:385–9.
[21] Qiu XH, Nazin GV, Ho W. Vibrationally resolved fluorescence excited with submolecular precision. Science 2003;299:542–6.
[22] Licari JJ, Hughes LA. Handbook of polymer coatings for electronics: Chemistry, technology and applications. Park Ridge, NJ: Noyes Publications; 1990.
[23] Senkevich JJ. Thickness effects in ultrathin film chemical vapor deposition polymers. J Vac Sci Technol A 2000; 18(5):2586–90.
[24] Giannelis EP. Polymer layered silicate nanocomposites. Adv Mater 1996;8(1):29.
[25] Vaia RA, Giannelis EP. Polymer nanocomposites: status and opportunities. MRS Bull 2001;26(5):394–401.
[26] Stillinger FH. A topographic view of supercooled liquids and glass-formation. Science 1995;267:1935–9.
[27] Ediger MD. Supercooled liquids and glasses. J Phys Chem 1996;100(31):13200–12.
[28] Debenedetti PG, Stillinger FH. Supercooled liquids and the glass transition. Nature 2001;410:259–67.
[29] Ediger MD. Spatially heterogeneous dynamics in supercooled liquids. Annu Rev Phys Chem 2000;51: 99–128.
[30] Jones RAL. The dynamics of thin polymer films. Curr Opin Colloid Interface Sci 1999;4(2):153–8.
[31] Forrest JA, Dalnoki-Veress K. The glass transition in thin polymer films. Adv Colloid Interface Sci 2001;94(1–3):167–96.
[32] Kas J, Strey H, Sackmann E. Direct imaging of reptation for semiflexible actin-filaments. Nature 1994;368:226–9.
[33] Perkins TT, Smith DE, Chu S. Direct observation of tube-like motion of a single polymer-chain. Science 1994;264: 819–22.
[34] Reilly PD, Skinner JL. Spectral diffusion of single molecule fluorescence: a probe of low-frequency localized excitations in disordered solids. Phys Rev Lett 1993;71:4257–60.
[35] Skinner JL, Moerner WE. Structure and dynamics in solids as probed by optical spectroscopy. J Phys Chem 1996; 100(31):13251–62.
[36] Geva E, Skinner JL. Theory of single-molecule optical line-shape distributions in low-temperature glasses. J Phys Chem B 1997;101(44):8920–32.
[37] Donley EA, Bach H, Wild UP, Plakhotnik T. Coupling strength distributions for dynamic interactions experienced by probe molecules in a polymer host. J Phys Chem A 1999;103(14):2282–9.
[38] Zumbusch A, Fleury L, Brown R, Bernard J, Orrit M. Probing individual two-level systems in a polymer by

correlation of single molecule fluorescence. Phys Rev Lett 1993;70:3584–7.
[39] Fleury L, Zumbusch A, Orrit M, Brown R, Bernard J. Spectral diffusion and individual 2-level systems probed by fluorescence of single terylene molecules in a polyethylene matrix. J Lumin 1993;56(1–6):15–28.
[40] Orrit M, Bernard J, Personov RI. High-resolution spectroscopy of organic-molecules in solids—from fluorescence line narrowing and hole-burning to single-molecule spectroscopy. J Phys Chem 1993;97(40):10256.
[41] Barkai E, Silbey R, Zumofen G. Lévy distribution of single molecule line shape cumulants in glasses. Phys Rev Lett 2000;84:5339–42.
[42] Bopp MA, Meixner AJ, Tarrach G, Zschokke-Granacher I, Novotny L. Direct imaging single molecule diffusion in a solid polymer host. Chem Phys Lett 1996;263(6):721–6.
[43] Bopp MA, Tarrach G, Lieb MA, Meixner AJ. Superresolution fluorescence imaging of single dye molecules in thin polymer films. J Vac Sci Technol A 1997;15(3):1423–6.
[44] Deschenes LA, Vanden Bout DA. Single molecule studies of heterogeneous dynamics in polymer melts near the glass transition. Science 2001;292:255–8.
[45] Deschenes LA, Vanden Bout DA. Molecular motions in polymer films near the glass transition: a single molecule study of rotational dynamics. J Phys Chem B 2001;105(48): 11978–85.
[46] Deschenes LA, Vanden Bout DA. Heterogeneous dynamics and domains in supercooled *o*-terphenyl: a single molecule study. J Phys Chem B 2002;106(44):11438–45.
[47] Ye JY, Ishikawa M, Yogi O, Okada T, Maruyama Y. Bimodal site distribution of a polymer film revealed by flexible single-molecule probes. Chem Phys Lett 1998; 288(5–6):885–90.
[48] Ishikawa M, Ye JY, Maruyama Y, Nakatsuka H. Triphenylmethane dyes revealing heterogeneity of their nanoenvironments: femtosecond, picosecond, and single-molecule studies. J Phys Chem A 1999;103(22):4319–31.
[49] Vallée RAL, Cotlet M, Hofkens J, De Schryver FC. Spatially heterogeneous dynamics in polymer glasses at room temperature probed by single molecule lifetime fluctuations. Macromolecules 2003;36(20):7752–8.
[50] Viteri CR, Gilliland JW, Yip WT. Probing the dynamic guest–host interactions in sol–gel films using single molecule spectroscopy. J Am Chem Soc 2003;12(7):1980–7.
[51] Bowden NB, Willets KA, Moerner WE, Waymouth RM. Synthesis of fluorescently labeled polymers and their use in single-molecule imaging. Macromolecules 2002;35(21): 8122–5.
[52] Vallée RAL, Tomczak N, Kuipers L, Vancso GJ, van Hulst NF. Single molecule lifetime fluctuations reveal segmental dynamics in polymers. Phys Rev Lett 2003; 91(3):038301.
[53] Hall DB, Underhill P, Torkelson JM. Spin coating of thin and ultrathin polymer films. Polym Eng Sci 1998;38(12): 2039–45.
[54] Lobo RFM, Pereira-da-Silva MA, Raposo M, Faria RM, Oliveira Jr ON. In situ thickness measurements of ultrathin multilayer polymer films by atomic force microscopy. Nanotechnology 1999;10(4):293–389.
[55] Ton-That C, Shard AG, Bradley RH. Thickness of spin-cast polymer thin films determined by angle-resolved XPS and AFM tip-scratch methods. Langmuir 2000;16(5):2281–4.
[56] Donley EA, Plakhotnik T. Luminescence lifetimes of single molecules in disordered media. J Chem Phys 2001;114(22): 9993–7.
[57] Basche T, Kummer S, Brauchle C. Direct spectroscopic observation of quantum jumps of a single-molecule. Nature 1995;373:132–4.
[58] Veerman JA, García-Parajó MF, Kuipers L, van Hulst NF. Time-varying triplet state lifetimes of single molecules. Phys Rev Lett 1999;83:2155–8.
[59] Zondervan R, Kulzer F, Orlinskii SB, Orrit M. Photoblinking of rhodamine 6G in poly(vinyl alcohol): radical dark state formed through the triplet. J Phys Chem A 2003;107(35):6770–6.
[60] Macklin JJ, Trautman JK, Harris TD, Brus LE. Imaging and time-resolved spectroscopy of single molecules at an interface. Science 1996;272:255–8.
[61] Vallée RAL, Tomczak N, Gersen H, van Dijk EMHP, García-Parajó MF, Vancso GJ, van Hulst NF. On the role of electromagnetic boundary conditions in single molecule fluorescence lifetime studies of dyes embedded in thin films. Chem Phys Lett 2001;348(3–4):161–7.
[62] Kreiter M, Prummer M, Hecht B, Wild UP. Orientation dependence of fluorescence lifetimes near an interface. J Chem Phys 2002;117(20):9430–3.
[63] Vallée RAL, Vancso GJ, van Hulst NF, Calbert JP, Cornil J, Bredas JL. Molecular fluorescence lifetime fluctuations: on the possible role of conformational effects. Chem Phys Lett 2003;372(1–2):282–7.
[64] Toptygin D. Effects of the solvent refractive index and its dispersion on the radiative decay rate and extinction coefficient of a fluorescent solute. J Fluorescence 2003; 13(3):201–19.
[65] Glauber RJ, Lewenstein M. Quantum optics of dielectric media. Phys Rev A 1991;43:467–91.
[66] Toptygin D, Savtchenko RS, Meadow ND, Roseman S, Brand L. Effect of the solvent refractive index on the excited-state lifetime of a single tryptophan residue in a protein. J Phys Chem B 2002;106(14):3724–34.
[67] Böttcher CJF. Theory of electric polarization, vol. 1: Dielectrics and static fields. Amsterdam: Elsevier Scientific; 1973.
[68] Nienhuis G, Alkemade CThJ. Physica 1976;81C:181.
[69] Rikken GLJA, Kessener YARR. Local field effects and electric and magnetic dipole transitions in dielectrics. Phys Rev Lett 1995;74:880–3.
[70] Schuurmans FJP, de Vries P, Lagendijk A. Local-field effects on spontaneous emission of impurity atoms in homogeneous dielectrics. Phys Lett A 2000;264(6):472–7.
[71] Simha R, Somcynsky T. On the statistical thermodynamics of spherical and chain molecule fluids. Macromolecules 1969;2(4):342–50.
[72] Adam G, Gibbs JH. J Chem Phys 1965;28:139.
[73] Bartko AP, Xu K, Dickson RM. Three-dimensional single molecule rotational diffusion in glassy state polymer films. Phys Rev Lett 2002;89:026101.
[74] Hall DB, Dhinojwala A, Torkelson JM. Translation–rotation paradox for diffusion in glass-forming polymers: the role of the temperature dependence of the relaxation time distribution. Phys Rev Lett 1997;79:103–6.

[75] Lindsey CP, Patterson GD. Detailed comparison of the Williams–Watts and Cole–Davidson functions. J Chem Phys 1980;73(7):3348–57.

[76] Blackburn FR, Cicerone MT, Hietpas G, Wagner PA, Ediger MD. Cooperative motion in fragile liquids near the glass-transition–probe reorientation in *o*-terphenyl and polystyrene. J Non-Cryst Solids 1994;172:256–64.

[77] Hooker JC, Torkelson JM. Coupling of probe reorientation dynamics and rotor motions to polymer relaxation as sensed by 2nd-harmonic generation and fluorescence. Macromolecules 1995;28(23):7683–92.

[78] Andreozzi L, Faetti M, Giordano M, Leporini D. Scaling between the rotational diffusion of tracers and the relaxation of polymers and glass formers. J Phys: Condens Matter 1999;11(10A):A131–7.